



Design and Implementation of a Textile-Based Embroidered Frequency Selective Surface

¹İbrahim Üner  0000-0002-4669-5894

²Sultan Can  0000-0002-9001-0506

¹Banu Hatice Gürcüm  0000-0001-9687-9598

²Asım Egemen Yılmaz  0000-0002-4156-4238

³Ertugrul Aksoy  0000-0002-6184-7112

¹Textile Desing Dept. Art and Desing Faculty of Ankara Hacı Bayram Veli University, Ankara, Türkiye

²Department of Electrical and Electronics Engineering, Ankara University, Ankara, Türkiye

³Department of Electrical and Electronics Engineering, Gazi University Ankara, Türkiye

Corresponding Author: İbrahim Üner, ibrahim.uner@hbv.edu.tr

ABSTRACT

This article presents the design, fabrication, and analysis of a textile-based band-stop frequency selective surface (FSS), in GSM, Wi-Fi, LTE, and WiMAX bands where the electromagnetic (EM) pollution is intense. The unit cell of the proposed FSS has been designed and simulated via a full-wave EM solver; CST Microwave Studio at the frequency of interest. In contrary to traditional FSS designs, which are printed on solid materials such as PCBs, this study presents an FSS considering a woven fabric as a substrate layer having features such as flexibility and compact weight. Two fabrication techniques have been considered one is conducted with a copper tape having a thickness of 35 µm denoted as CT FSS and the second one is conductive yarn embroidering technique denoted as CY FSS for the conducting pattern. Fabricated samples are evaluated in terms of transmission characteristics and a satisfactory agreement is obtained between CT FSS and CY FSS for both simulations and fabricated prototypes.

1. INTRODUCTION

Increasing demand on using electronic devices in our daily routine gave a rise on using the particular frequency bands, such as GSM (including 2G, 3G, LTE, and LTE-advanced sub-bands), Bluetooth, and Wi-Fi / Wi-Max in the wireless networks [1–3] and EM field emitting devices. Spotlight on these bands caused electromagnetic pollution since the devices have to satisfy the increasing demands of the users regarding high speed, large coverage, mobility, propagation, transmission power, spectrum efficiency, safety, and security [4–7]. The literature conveys significant amount of research on electromagnetic pollution [8], especially on electromagnetic interference (EMI). EMI which is a serious problem to cope with since it may cause electrical and electronic malfunctions, can prevent the proper use of the

radio frequency spectrum, can ignite flammable or other hazardous atmospheres [9], and more importantly can endanger human health [6, 9]. The evaluation of its side effects on human health has attracted many interests in medical studies, especially for people suffering from electromagnetic hypersensitivity [10], for environmental exposure to RF radiation [11, 12], and the measurement of electromagnetic radiation [12–19]. Consequently, EMI shielding, defined as the prevention of the propagation of EM waves from one region to another by using shield materials [20], is crucial to hinder those problems and to protect human beings and sensitive appliances.

To reduce the EMI [21], or to eliminate interference in desired frequencies [5], frequency selective surfaces (FSS) are used extensively in electromagnetic shielding

To cite this article: Üner İ, Can S, Gürcüm BH, Yılmaz AE, Aksoy E. 2022. Design and implementation of a textile-based embroidered frequency selective surface. *Tekstil ve Konfeksiyon* 32(4), 297-303.

ARTICLE HISTORY

Received: 26.01.2021

Accepted: 14.09.2021

KEYWORDS

Conductive yarn, electromagnetic textile, embroidery, EMI shielding fabric, frequency selective surface

applications. They are periodic structures with conductive unit cell element arrays (patches or cavities) arranged on a dielectric substrate in any periodicity, any lattice, and any shape. FSSs can be designed as a band-pass or band-stop filter. The responses of their surface transmission and reflection on incident electromagnetic waves depend on the geometry and material properties of the unit cell as well as the periodicity [22]. Especially FSSs with the band-stop filter characteristics have the property of preventing the undesired interferences and transmitting the selected signals at a particular frequency simultaneously [23, 24]. FSS designs have widespread application area including enhancing the efficiency of the smart houses, which are getting popular since people demand amenity and comfort in the last few decades [21]. With these shielding characteristics, FSSs are used as radar absorption materials, radome design, and antennas [5].

In electronic and communications engineering, several EMI-shielding or EM-absorbing issues have been studied for decades. These can be summarized as; shielding effectiveness measurements [25], metamaterials, specialized materials used for shielding enclosures [26], conduction mechanisms, problems on waveguide aperture and ventilation [27], dielectric materials for absorber applications [28], electromagnetic wave absorbers [29, 30]. However, in the field of textile engineering EMI shielding and frequency selective surface (FSS) metamaterials are the most recent topics [5, 31].

All shielding materials must meet required specifications in chemical and corrosion resistance, tunable morphology, ease of operation, and financial cost [32, 33]. Besides these requirements, two basic demands urge the use of shielding material designs; one is weight reduction or lightweight, which reasons the employment of lighter materials such as aerogels [20], foam-based materials [34], magnetic nanoparticles [35], conductive polymer composites [36], and conductive textiles [37] within the fabrication process of shielding materials. The second is the demand for flexible designs implemented on curved platforms for any shielding applications. So, the development of electronics and material science leads the path to the scope of textile formation techniques making textile a research area in EMI shielding or FSS design. The studies proposed in literature emphasizes, conductivity is critical for EMI shielding of textiles [38]. Therefore, metal fibers, copper, or silver wires are used in spinning processes. Conductive dyes or solutions are applied to fabrics. For instance, to obtain a multilayered composite cloth structure against EMI, copper-coated interlining fabric and other textile components are sandwiched together to get composite EMI shielding fabric [39]. In another study, the EMSE (electromagnetic shielding effectiveness) values of copper plate and copper composite woven and knitted fabrics were compared [40]. In the study, PA6/silver mixture was used to investigate the EM shielding property of electrospun

nanofibers [41]. For technical textile application, kevlar/stainless steel/polyamide fibers composite knitted specimens were tested at the frequency band of 0-3000 MHz [37].

The studies about shielding are focusing on the EMSE value, reaching an acceptable EMSE value in the relevant frequency range is mostly the main aim of the studies. Previous studies on EM shielding textiles, such as woven and knitted fabrics, generally indicate the effect of weaving or knitting structure and metal density in textiles [42]. Dielectric properties of textiles are not taken into account in EMI shielding studies. Also simulation studies based on EM wave theories are not needed before the experimental study. However, FSSs show EM filter behavior by stopping or passing EMI at the relevant frequency (e.g., 2.45 GHz).

This study presents a novel textile based FSS design fabricated with embroidering technique. The study includes the analysis of the band-stop characteristics of the proposed frequency selective surface denoted as Conductive Yarn (CY) FSS. The prototype CY FSS was fabricated, measured, and validated via the conventional band-stop frequency selective surface conducted with a copper tape denoted as CT FSS. The designs and simulations of the unit cells were carried out via a full-wave EM solver (CST Microwave Studio) at the frequency of interest. Samples were evaluated in terms of transmission characteristics (S21).

2. MATERIAL AND METHOD

In this article, band-stop FSS was designed for the frequencies of GSM, LTE, Wi-Fi, and WiMAX bands and simulated with a full-wave electromagnetic simulator, CST Microwave Studio. The EM wave filtering performances of FSSs were calculated, designed, and simulated by numerical method and produced with copper tapes onto cotton and cotton / PES blend fabrics. To create more flexible and durable textile-based FSS, conductive yarn was employed by embroidery technique subsequently and compared with simulations.

2.1 Material

FSS designs consists of conducting patches or cavities etched on the dielectric layer depending on the aim on blocking or passing the EM waves. The dielectric layers are commonly rigid and inflexible materials and patches are made of a thin copper plate as shown in Figure 1.

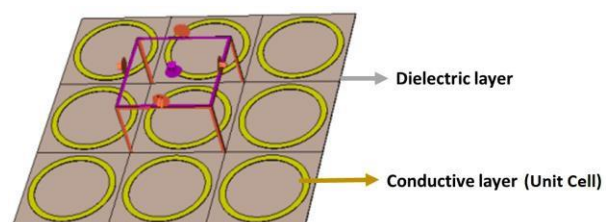


Figure 1. Conventional FSS structure

In the novel design proposed in this study, woven fabrics were used as a dielectric layer and embroidered conductive yarn was patterned as a conductive layer (unit cell). Since previous research has proven that plain woven fabrics are having a good agreement with the designs, three samples (F1, F2, F3) are chosen plain woven with different thicknesses, weights, and setts together with only one twill woven (F4) sample. The physical properties of woven fabrics used for designs are presented in Table 1.

Table 1. Physical properties of textile materials

Code	Structure	Materials	Thickness	g/m ²	Warp yarn. cm-1	Weft yarn. cm-1
F1	Plain 1/1	Cotton	0.6 mm	300	14	10
F2	Plain 1/1	Cotton	0.53 mm	170	17	17
F3	Plain 1/1	Cotton	0.40 mm	150	22	14
F4	Twill 2/2 S	Cotton/PES	0.55 mm	220	45	24

The first design, referred to as “CT FSS” standing for “copper tape FSS” is fabricated by agglutinating 35µm copper tape as a conductive layer on the fabric substrate in-house. On the other hand, the second design, referred to as “CY FSS” standing for “conductive yarn FSS” is fabricated by Shieldex Statex (117d/f17-2 ply) conductive yarn as a unit cell on a fabric substrate.

2.2 Method

2.2.1 Measurement of dielectric values of fabrics

The dielectric values of the woven fabrics are important to ensure filtering at the relevant frequencies. For this reason, the dielectric values of the fabric substrates are measured. In this study, the permittivity of the textile materials has been extracted employing Keysight 85070E Dielectric Probe Kit in the frequency interval 500-3000 MHz.

2.2.2 Unit-cell design and numerical results for the proposed FSS

Since free space measurements requires mass production of the unit cell designs for simplicity on measuring procedure waveguide measurement set up has been preferred for conducting the studies. For that aim both simulation and measurement setup for analyzing the unit cell responses Pasternack WR-229 waveguide (2.29 inches [58.166 mm] x 1.145 inches [29.083 mm]) having a frequency range of 3.3 GHz to 4.9 GHz is used. This waveguide is selected in particular since it satisfies the requirements for the band of interest as well as having low loss RF transmission lines capable of handling high power with high isolation. Since the unit cell is designed according to the measurement set up (WR-229 waveguide measurement set up), for ensuring the alignment, the side lengths of the unit cell are defined as having a length value of L_{wg} and a width value of W_{wg} so the unit cell fit in the waveguide perfectly. The textile

substrate having a thickness value of H_s is considered as the substrate having the permittivity value of ϵ_r and the resonator pattern is proposed in Figure 2.

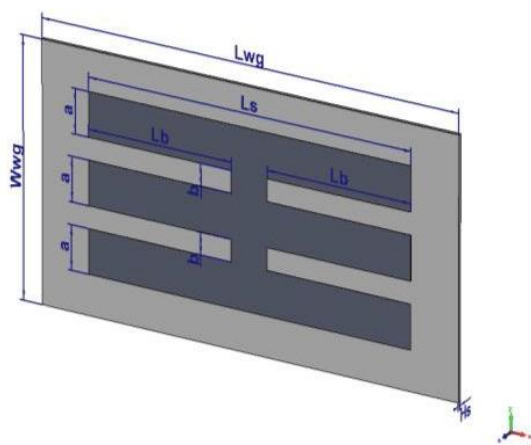


Figure 2. Unit cell design of FSS with its parameters

As shown in Figure 2, the textile dielectric substrate is represented with the light grey part of the unit cell and the dark grey part represents the conductor material having the dimensions of L_s , a , b and L_b . The optimized unit cell has the dimensions of $L_{wg} = 58.17$ mm, $W_{wg} = 29.08$ mm, and $H_s = 0.5$ mm. Resonator dimensions L_s , L_b , a , and b are given as 45 mm, 20 mm, 5 mm, and 2.5 mm, respectively. The boundary conditions are assigned as electric boundary conditions on the x and y axes and open boundaries on the z-axis. As a port assignment, a waveguide port is assigned.

2.2.3 Embroidery process of FSS unit cell

The embroidery technique was used for the production of FSS and the patterns were created with the PFAFF Creative 1.5 embroidery machine. Shieldex Statex 117 / f 17 2 plies conductive yarn was used in the formation of the conductive patch. The optimized FSS unit cell was drawn in the premier + embroidery software and transferred to the embroidery machine (Figure 3a-b-c). The embroidery density applied in the study includes 154 punch / cm² in complex fill and a total of 1396 punch and punch angle is 450 within the FSS design.

Today, embroidery design can be done with CAD systems, which provides unlimited patterning possibilities with embroidery technique. This technological advance has made it possible for digital images to be directly embroidered using a computer-aided embroidery machine.

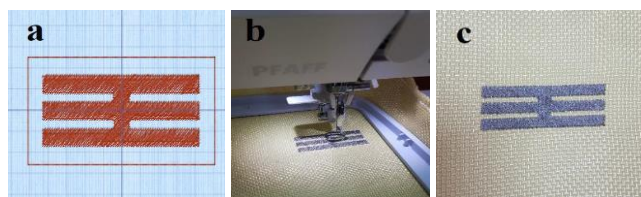


Figure 3. CY FSS (a) patterning of FSS on Premier + software, (b) embroidery process of FSS, (c) embroidered FSS

2.2.4 Measurement set-up

S-parameters ($|S_{11}|$, $|S_{12}|$, $|S_{21}|$, $|S_{22}|$) Considered for evaluating the band stop and band pass characteristics of the fabricated samples. $|S_{11}|$ (magnitude of reflection coefficient) indicates how much electromagnetic waves are reflected from the medium, $|S_{21}|$ (transmission coefficient) indicates how much electromagnetic waves are transmitted through a medium [14]. In this study, $|S_{21}|$ is the key parameter For the evaluation of the band characteristics of the proposed designs. Pasternack WR-229 waveguide having a frequency range of 3.3 GHz to 4.9 GHz is connected to Rohde & Schwarz ZVL13 Vector Network Analyzer, which is capable of measuring a frequency interval of 9 kHz - 13.6 GHz, is used throughout the measurements and the cross-section of the waveguide is shown in Figure 4.

The unit cell simulation is mimicked throw-out the measurement set up and the sample is located at the midpoint of the waveguide by using foams. The foams are critical in satisfying the stability and they are having approximate permittivity and permeability values of air so that it has a negligible effect on measuring the scattering parameters; however, it helps to sample to stay firm.

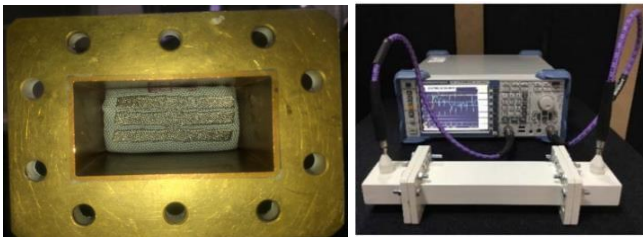


Figure 4. One of the proposed sample in the WR-229 rectangular waveguide

3. RESULTS AND DISCUSSION

3.1. Measurement of dielectric values of fabrics

The dielectric properties of four different textile samples (F1, F2, F3, F4) within the scope of the study were examined between 500 MHz and 3000 MHz. ϵ' values for each fabric sample were measured 3 times (M1, M2, and M3 are corresponding to the first, second, and third measurements, respectively) and tested at 201 different frequencies scaled between 500 MHz and 3000 MHz with an accuracy of 12.5 MHz. Accordingly, while the maximum ϵ' values occurred at 537.5 MHz in all samples, the minimum ϵ' values were observed at 950 MHz in all samples except F1 which peaked at 2287.5 MHz for minimum ϵ' .

As presented in Figure 5, the dielectric coefficients decrease as the frequency increase in all fabric types. In the dielectric studies of textiles in the literature [43–48], it is seen that external factors such as humidity, temperature, and frequency range affect the measured values. In this respect, there is a concordance between our study and the literature. Moreover, the result of an inverse relationship between the frequency increase and the dielectric coefficient has been revealed. In reviewing the literature, no data was found on the association between frequency and dielectric coefficient of textiles, hence it maybe contribution to literature. Although the resonance dependent dielectric tendency of the F1, F2, and F3 was similar, each sample did not show exactly the same dielectric properties due to the differences in the physical properties (thickness, weight, and sett values) of the fabrics.

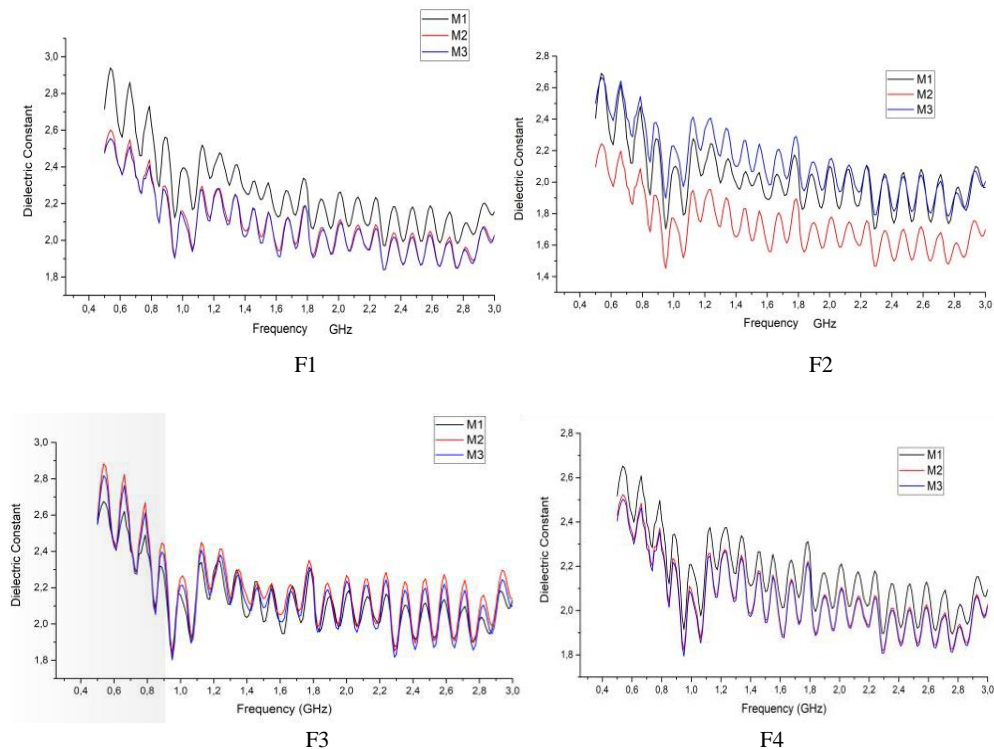


Figure 5. Relative Permittivity values of samples (see Table 1) depending on the frequency

3.2 Measurement results of FSS

The effect of the dielectric coefficient on the frequency is seen in the simulation study performed by taking into account the maximum and minimum ϵ_r' values of the fabrics under test (Figure 6).

Firstly, proposed textile-based structures were compared as a function of minimum and maximum ϵ_r' values depending on frequency. In Figure 6, when the ϵ_r' value increased, the resonance frequency shifted to the down side. Thus, the conclusion can be drawn that the dielectric permittivity of fabrics affects the resonance frequency of FSS. This finding is consistent with [49]'s statement, which gives information about permittivity.

According to Figure 6, the corresponding upper and lower frequencies of F1 are 4.19 GHz and 3.74 GHz for the

simulations as a function of ϵ_r' and 4.19 GHz for the CT FSS measurement respectively. For F2, the resonance frequencies are 4.38 GHz and 3.79 GHz for the simulations, and 4.38 GHz for CT FSS. The resonance frequencies of F3 are 3.76 GHz and 3.56 GHz for the simulations, and 4.47 GHz for CT FSS. For F4, 4.31 GHz, and 3.93 GHz for simulations and 4.28 GHz for the CT FSS measurement. The % error fr calculated via equation (1) based on minimum ϵ_r' is lower than 1% compared to copper tape, except F3. Therefore, it was stated that the measurements of the CT FSS samples, except F3, matched quite well with the minimum ϵ_r' simulation results. For this reason, it was decided to use F1 and F4 fabrics in the CY FSS fabrication phase of the study.

$$\% \text{ Error } fr = \left(\frac{fr \text{ simulated} - fr \text{ measured}}{fr \text{ simulated}} \right) \times 100 \quad (1)$$

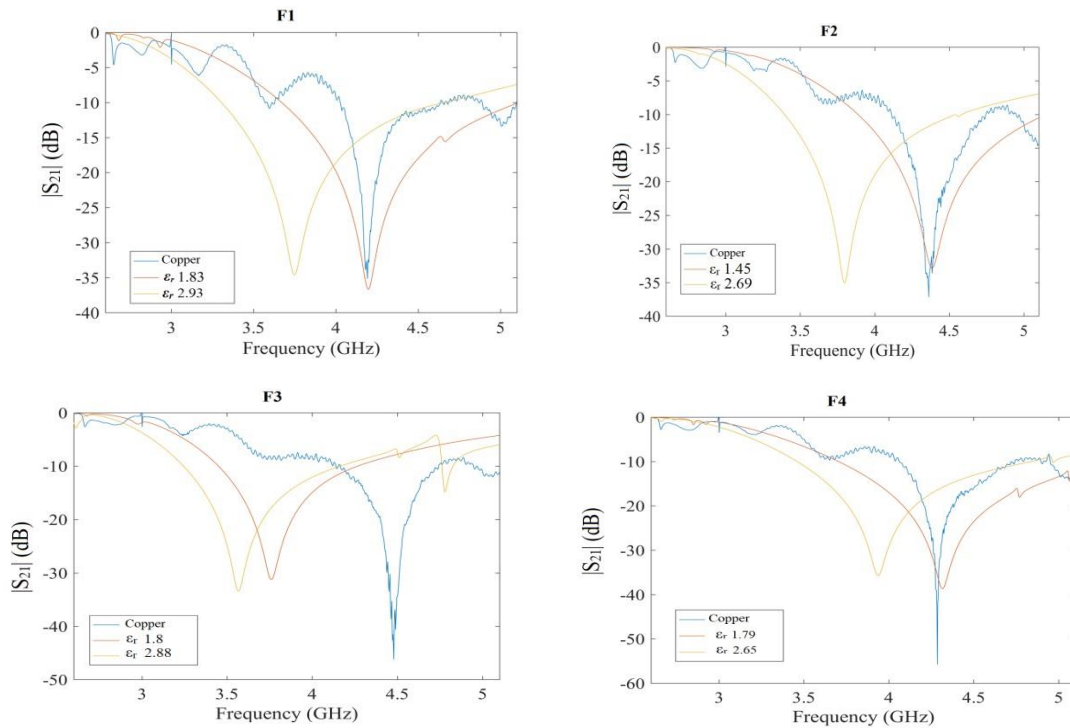


Figure 6. $|S_{21}|$ characteristics for CT FSS a) simulations and CT measurements

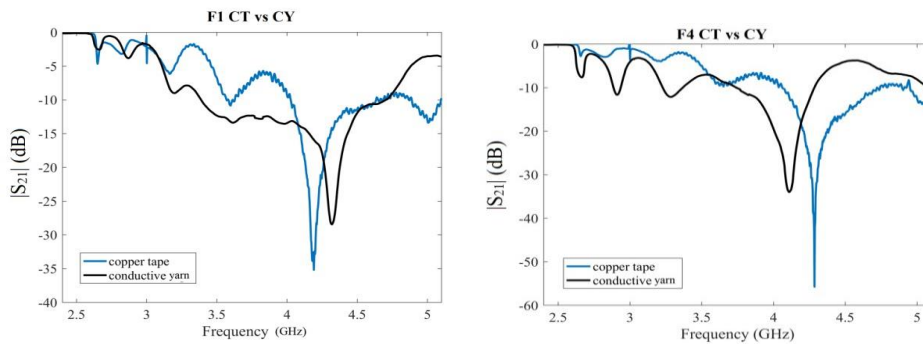


Figure 7. Measurement of CT FSS and CY FSS Resonance frequencies and $|S_{21}|$ (dB) values of F1 and F4

The good results of CT FSS measurements compared to simulation results have provided the opportunity to use textiles as a dielectric layer in FSSs. There are similarities between the attitudes expressed by [10] in this study and those described by us. Since the copper tapes used in CT FSS are not as flexible as the fabric and resistant to environmental conditions such as rubbing, wetting, bending, and folding, the FSS unit cell is produced with conductive yarn to solve these problems. The embroidered unit cell structures (CY FSS) are more compatible with the textile structure and more flexible and durable than CT FSS. The results of CT FSS and CY FSS were compared in Figure 7. Accordingly, the conductive yarn results for F1 are 4.3208 GHz and -28.46 dB, while the copper tape results are 4.1918 GHz and -35.2 dB, respectively. The conductive yarn results for F4 are 4.11 GHz and -34.01 dB, while the copper tape results are 4.2858 GHz and -55.77 dB, respectively. As can be seen from figure 7, there is a slight frequency difference between CT FSS and CY FSS, while transmission coefficients are acceptable (under -10 dB) in both. This also accords with the researchers' earlier observations, which showed that there are differences between simulation/copper and textile FSS [10, 50, 51].

4. CONCLUSION

This project was undertaken to design a textile-based EM filter and evaluate its filtering performance versus its rigid counterpart. To eliminate the weightiness and stiffness disadvantages of conventional FSS, four different fabric

structures were designed as the dielectric layer and the unit cell was fabricated by copper tape (CT FSS) and conductive yarn (CY FSS). To design FSS, the dielectric permittivity of four different fabrics was tested between 500 MHz and 3000 MHz with 12.5 MHz accuracy.

The conclusion can be drawn that the dielectric permittivity is dependent on the physical properties of the textile and has an effect on the resonance frequency as well as the geometric structure of the conductive surface (unit cell). Also, as the dielectric value increases, the resonance frequency of the FSS decreases.

Measurements of CT FSSs made by agglutinated copper tape onto fabric are well-matched with simulations because of the perfectness of the unit cell geometry. However, the inflexibility of copper tape and its weakness against environmental factors constitute a disadvantage. The unit cell produced with conductive yarn is thought to be a better fit with the textile dielectric layer due to the embroidery technique. The experimental results of CY FSS have been compared to CT FSS and satisfactory agreement is obtained.

As a result of this study, it can be concluded that the embroidery samples are having approximate performance in terms of filtering and they are good candidate for EM filter applications. To increase the efficiency of the embroidery technique in this regard, researches on embroidery parameters such as stitch density, surface filling method, and stitch slope will yield positive results.

REFERENCES

- Zulkifli CZ, Hassan HN, Ismail W, Semunab SN. 2015. Embedded RFID and wireless mesh sensor network materializing automated production line monitoring. *Acta Physica Polonica A*. 128 (2B), 86-89.
- Basit A, Qureshi IM, Khan W, Malik AN. 2016. Range-angle-dependent beamforming for cognitive antenna array radar with frequency diversity. *Cognitive Computation*. 8(204), 204-2016.
- Mukanova B, Mirgalikyzy T. 2015. Simulation of the electric field of a point source on the relief surface. *Acta Physica Polonica A* 128(2B), 142-144.
- Karan Y, As N, Şahin ME. 2017. Investigation of GSM, LTE and WI-FI electromagnetic radiation in dwellings. *Acta Physica Polonica A* 132(3), 509-512.
- Can S, Karakaya EU, Yılmaz AE. 2020. Design, fabrication, and measurement of textile-based frequency selective surfaces. *Microwave and Optical Technology Letters*. DOI: 10.1002/mop.32474.
- Eurocontrol, "Criteria for selection of frequency band(s) for the future aeronautical communication infrastructure," 2005. [Online]. Available: [https://www.icao.int/safety/acp/ACPWGF/ACP-WG-F-13/WP36-Band Selection criteria for AI 1\[1\].6 ITU.doc](https://www.icao.int/safety/acp/ACPWGF/ACP-WG-F-13/WP36-Band%20Selection%20criteria%20for%20AI%201%201.6%20ITU.doc).
- Velentza O. 2015. Electromagnetic pollution - pathological effects of electromagnetic fields in man. *AASCIT Journal of Health*.2(6) 74-79.
- Richman R, Munroe AJ, Siddiqui Y. 2014. A pilot neighborhood study towards establishing a benchmark for reducing electromagnetic field levels within single family residential dwellings. *The Science of the Total Environment*. 466, 625-634.
- Tan K-S, Hinberg I. 2004. Electromagnetic interference with medical devices: in vitro laboratory studies and electromagnetic compatibility standards. In Biomedical Engineering. Editor: Dyro J F, *Clinical Engineering Handbook*, Academic Press, 254-262.
- Hesarian MS, Shaikhzadeh NS, Sarraf SR. 2018. Design and fabrication of a fabric for electromagnetic filtering application (experimental and modeling analysis). *The Journal of the Textile Institute* (109), 775-784.
- Ayinmode BO, Farai IP, Pacific J. 2014. Evaluation of GSM radiation power density in three major cities in Nigeria. *International Journal of Environmental and Ecological Engineering* 8(10), 740 - 743.
- Seyfi L. 2013. Measurement of electromagnetic radiation with respect to the hours and days of a week at 100kHz-3GHz frequency band in a Turkish dwelling. *Measurement* 46(9), 3002-3009.
- Cansiz M, Abbasov T, Kurt MB, Çelik AR. 2016. Mobile measurement of radiofrequency electromagnetic field exposure level and statistical analysis *Measurement* 86, 159-164.

14. As N, Dilek B, Şahin ME, Karan Y. 2014. Electromagnetic pollution measurement in the RTE university campus area *Global Journal on Advances Pure and Applied Science* 3, 65.
15. Urbinello D, Joseph W, Huss A, Verloock L, Beekhuizen J, Vermeulen R, Martens L, Rööslı M. 2014. Radio-frequency electromagnetic field (RF-EMF) exposure levels in different European outdoor urban environments in comparison with regulatory limits *Environ International* 68, 49.
16. Sahin ME, As N, Karan Y. 2013. Selective radiation measurement for safety evaluation on base stations *Gazi University Journal of Science* 26(1), 73-83.
17. Eyübođlu E, Kaya H. 2010. December. Measurement of TV/radio transmitters at Trabzon-Boztepe region induced electric field strength and evaluation of results. In: Electrical, Electronics and Computer Engineering Editor (Ed) IEEE , (ELECO) 2010 2010 National Conference on Electrical, Electronics and Computer Engineering Bursa, Turkey.
18. Henderson SI, Bangay MJ. 2005. Survey of RF exposure levels from mobile telephone base stations in Australia. *Bioelectromagnetics Journal* 27, 73.
19. Akkurt I, Mavi B. 2010. The measurement of radiation dose around base-stations. *Scientific Research and Essays* 5(15), 2088-2090.
20. Zhang L, Bi S, Liu M. 2019. Lightweight electromagnetic interference shielding materials and their mechanisms, *Electromagnetic Materials and Devices*. 1–20.
21. Can S, Kapusuz KY, Yılmaz AE. 2017. Optically transparent frequency selective surface for ultra-wideband applications. *Microwave and Optical Technology Letters* 59 (12), 3198-3200.
22. Munk BA. 2000. *Frequency Selective Surfaces: Theory and Design*. Hoboken, NJ, USA: John Wiley & Sons, Inc. DOI: 10.1002/0471723770.
23. Karahan M, Aksoy E, Yavuz YA. 2017. June. Frequency selective surface design to reduce the interference effect on satellite communication. In IEEE, 8th International Conference on Recent Advances in Space Technologies (RAST), 221–223. Istanbul, Turkey.
24. Karahan M, Aksoy E. 2020. Design and analysis of angular stable antipodal F-type frequency selective surface with multi-band characteristics. *International Journal of RF and Microwave Computer Aided Engineering* (30), 1-16.
25. Fang CH, Zheng SQ, Tan H, D. Xie G, Q Zhang, 2008. Shielding effectiveness measurements on enclosures with various apertures by both mode-tuned reverberation chamber and GTEM cell methodologies, *Progress In Electromagnetics Research B* 2, 103–114.
26. Atxaga G, Marcos J, Jurado M, Carapelle A, Orava R. 2012 October. Radiation shielding of composite space enclosures, 63rd International Astronautical Congress, Naples, Italy.
27. Li M, Nuebel J, Drewniak JL, DuBroff RE, Hubing TH, Van Doren TP. 2000. EMI from airflow aperture arrays in shielding enclosures—experiments, FDTD, and MoM modeling, *IEEE Transactions on Electromagnetic Compatibility* 42(3), 265–275.
28. Hamat Ö. 2014. Design and development of electromagnetic wave absorbing composites effective at microwave frequencies Middle East Technical University, (Master's Thesis) Department of Metallurgical and Materials Engineering, Ankara.
29. Costa F, Monorchio A, Manara G. 2016. Theory, design and perspectives of electromagnetic wave absorbers. *IEEE Transactions on Electromagnetic Compatibility* 5(2), 67–74.
30. Watts C, Liu X, Padilla W. 2012. Metamaterial electromagnetic wave absorbers. *Advanced Optical Materials* 24(23) 98-120.
31. Michalak M, Brazis R, Schabek D, Krucińska I. 2019 June. Textile metamaterials, in AUTEX 2019-19th World Textile Conference on Textiles at the Crossroads, Ghent, Belgium.
32. Gairola P, Gairola SP, Dhawan SK, Tandon RP, Gupta V, Purohit LP, Sharma S. 2018. Carbon material-nanoferrite composite for radiation shielding in microwave frequency, *Integrated Ferroelectrics* 186(1), 40–48.
33. Gonzalez M, Pozuelo J, Baselga J. 2018. Electromagnetic shielding materials in GHz range. *The Chemical Record* 8(7–8), 1000–1009.
34. Wang YY, Zhou ZH, Zhou CG, Sun WJ, Gao JF, Dai K, Yan DX, Li ZM. 2020. Lightweight and robust carbon nanotube/polyimide foam for efficient and heat-resistant electromagnetic interference shielding and microwave absorption. *ACS Applied Materials & Interfaces* 12(7), 8704-8712.
35. Parveen S, Veena C, Vijayan N, Kotnala RK. 2012. Improved electromagnetic interference shielding response of poly(aniline)-coated fabrics containing dielectric and magnetic nanoparticles. *The Journal of Physical Chemistry C* 116(24), 13403-13412.
36. Valente R, De Ruijter C, Vlasveld D, Van Der Zwaag S, Groen P. 2017. Setup for EMI shielding effectiveness tests of electrically conductive polymer composites at frequencies up to 3.0 GHz. *IEEE Access* (5), 16665-16675.
37. Demıray Soyaslan D. 2020. Design and manufacturing of fabric reinforced electromagnetic shielding composite materials. *Tekstil ve Konfeksiyon*, 30(2), 92-98.
38. Çetiner S, Köse HA. 2021. Systematic study on morphological, electrical and electromagnetic shielding performance of polypyrrole coated polyester fabrics. *Tekstil ve Konfeksiyon* 31(2), 111-121.
39. Şaravanja B, Malarić K, Pušić T, Ujević D. 2020. Exposure analysis of electromagnetic shield effect of a copper composite cloth structure. *Tekstil ve Konfeksiyon* 30(2), 139-143.
40. Özkan İ. 2020. Investigation on the electromagnetic shielding performance of copper plate and copper composite fabrics: A comparative study. *Tekstil ve Konfeksiyon* 30(2), 156-162.
41. Sancak E, Özen MS, Erdem R, Yılmaz AC, Yüksek M, Soin N, Shah T. 2018. PA6/silver blends: Investigation of mechanical and electromagnetic shielding behavior of electrospun nanofibers. *Tekstil ve Konfeksiyon* 28 (3), 229-235.
42. Örtlek HG, Güneşođlu C, Okyay G, Türkođlu Y. 2012. Investigation of electromagnetic shielding and comfort properties of single jersey fabrics knitted from hybrid yarns containing metal wire. *Tekstil ve Konfeksiyon* 2012 (2), 90-101.
43. Ibanez-Labiano I, Alomainy A. 2020. Dielectric characterization of non-conductive fabrics for temperature sensing through resonating antenna structures. *Materials* (13), 1271.
44. Sankaralingam S, Gupta B. 2010. Determination of dielectric constant of fabric materials and their use as substrates for design and development of antennas for wearable applications. *IEEE Transactions on Instrumentation and Measurement* (59), 3122– 3130.
45. Mustata FC, Mustata A. 2014. Dielectric behaviour of some woven fabrics on the basis of natural cellulosic fibers. *Advances in Materials Science and Engineering* (2014).
46. Lesnikowski J. 2012. Dielectric permittivity measurement methods of textile substrate of textile transmission lines. *Przełąd Elektrotechniczny* (88), 148-151.
47. Pourouva M, Zajicek R, Oppl L. 2008, April. Measurement of dielectric properties of moisture textile. In: 2008 14th Conference on Microwave Techniques. 1–4. Prague, Czech Republic.
48. Cerovic DD, Asanovic KA, Maletic SB. 2013. Comparative study of the electrical and structural properties of woven fabrics. *Composites Part B: Engineering* (49), 65–70.
49. Delihanlar E, Yüzer AH. 2020. Wearable textile fabric based 3D metamaterials absorber in X-band. *Applied Computational Electromagnetics Society Journal* 35 (2), 230–236.
50. Alonso-Gonzalez L, Ver-Hoeye S, Fernandez-Garcia M. 2018. Layer-to-layer angle interlock 3D woven band stop frequency selective surface. *Progress in Electromagnetics Research* (162), 81–94.
51. Guan F, Xiao H, Shi M. 2017. Realization of planar frequency selective fabrics and analysis of transmission characteristics. *Textile Research Journal* (87), 1360–1366.